

Random laser action in self-organized para-sexiphenyl nanofibers grown by hot-wall epitaxy

F. Quochi,^{a)} F. Cordella, R. Orrù, J. E. Communal, P. Verzeroli, A. Mura, and G. Bongiovanni

Dipartimento di Fisica, Università di Cagliari and Istituto Nazionale per la Fisica della Materia I-09042 Monserrato (CA), Italy

A. Andreev, H. Sitter, and N. S. Sariciftci

Institute for Semiconductor and Solid State Physics and Linz Institute for Organic Solar Cells (LIOS), Physical Chemistry at the Johannes Kepler University Linz, A-4040 Linz, Austria

(Received 31 October 2003; accepted 12 April 2004; published online 12 May 2004)

We report on the observation of amplified spontaneous emission and random lasing in self-organized crystalline *para*-sexiphenyl nanofibers. Using subpicosecond excitation, a lasing threshold is observed on the 0–1 emission band near 425 nm at excitation fluences as low as $0.5 \mu\text{J}/\text{cm}^2$ ($6 \times 10^{16} \text{ cm}^{-3}$ equivalent density), near the onset of density-dependent recombination processes. The dependence of the nonlinear emission spectrum on both the pump intensity and position of the excitation area are attributed to the interplay between random lasing and amplified spontaneous emission occurring along the nanofibers. © 2004 American Institute of Physics.

[DOI: 10.1063/1.1759384]

Conjugated polymers and oligomers have become increasingly interesting materials for applications in different optoelectronic devices, such as field-effect transistors, photovoltaic cells, light-emitting diodes, and potentially, laser diodes. In the perspective to achieve electrical pumping in light-amplifying organic devices, the research on new organic active materials has been focused on the study of amplified spontaneous emission (ASE) and lasing processes with photopumping techniques. ASE and laser action have been reported so far in a number of polymeric and dye-doped organic thin films embedded in optical waveguides with different solutions for the laser cavity mirrors.^{1–4} Oligomers offer clear advantages over polymers for applications involving highly ordered structures. ASE has been observed in oligo-thiophene,⁵ oligo-(phenylene vinylene),⁶ and related co-oligomer⁷ single crystals; however, it has not been reported in the case of polycrystalline films with small domains, due to high optical losses occurring at the interfaces between different grain domains.⁶ In recent years, various groups have fabricated self-organized crystalline nanofibers of oligo-phenylenes with the potential for future applications in photonics as nanoscale laser sources.^{8–10} Investigations of the nonlinear optical response of oligo-phenylene nanofibers have shown so far only evidence of spectral narrowing.¹¹

In this letter, we report on the observation of random laser action in crystalline *para*-sexiphenyl (*p*-6P). Crystalline nanofibers of *p*-6P are grown by hot-wall epitaxy (HWE) on freshly cleaved mica substrates, under a dynamic vacuum of 10^{-6} mbar, at a substrate temperature of 130 °C. Under these conditions, *p*-6P molecules self-organize in very long (more than $\approx 100 \mu\text{m}$)⁹ needle-shaped nanofibers, which in turn consist of crystalline domains showing three different epitaxial relationships to the mica substrate.¹² Importantly, the alignment of the *p*-6P long molecular axes is

nearly the same in all domains—practically parallel to the substrate and perpendicular to the fiber direction.^{9,12} Such a uniform alignment of molecules reflects in very high dichroic ratios of *p*-6P nano-fibers—up to 14 in absorption and emission,⁹ as well as in waveguiding behavior of single nanofibers.¹³

Samples with different quantities of deposited material are grown, resulting in nanofibers with different average heights, ranging from 100 to 400 nm. The *p*-6P nanocrystals are photoexcited with the frequency-doubled pulses (at 380 nm) of a Ti:Sapphire regenerative amplifier delivering 150 fs long pulses at 1 kHz repetition rate. Laser spot sizes of $\approx 120 \mu\text{m}$ (diameter) are used for photoexcitation. The samples are mounted in a recirculating-loop cold-finger cryostat for low-temperature measurements. The optical emission is collected at different angles with respect to the normal to the substrate, then dispersed in a 46 cm single spectrometer and detected by a cooled charge-coupled device.

Figure 1 shows the surface morphology of the sample used to obtain the results presented in this letter. A line profile made nearly diagonally (so as to intersect the fibers perpendicularly) shows an average base width $\langle b \rangle$ and height

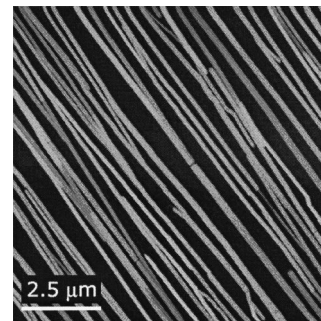


FIG. 1. $10 \times 10 \mu\text{m}$ AFM topography image of the surface morphology of a *p*-6P film grown by HWE at 130 °C on mica.

^{a)}Electronic mail: francesco.quochi@dsf.unica.it

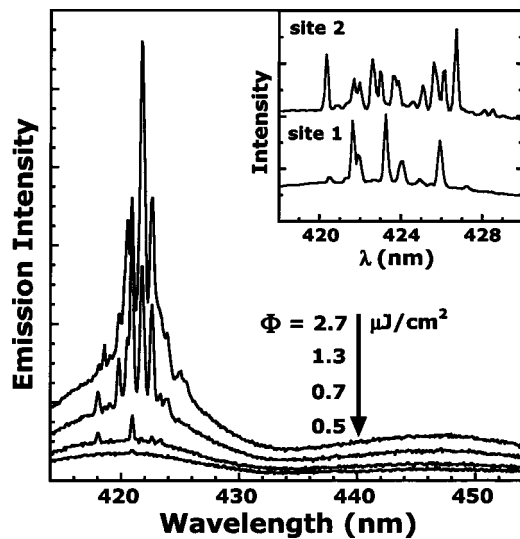


FIG. 2. Main panel: Emission spectra taken at different values of the pump fluence Φ ($\mu\text{J}/\text{cm}^2$ per pulse) at $T=30$ K. Inset: Emission spectra measured in two different positions across the sample surface at the same excitation level above threshold ($T=300$ K).

$\langle h \rangle$ of the nanofibers of about 220 nm and 110 nm, respectively. The fraction of substrate surface covered with fibers is estimated to be $\approx 50\%$. Based on the results of recent calculations of the propagation modes of p -6P waveguides,¹³ we hereafter assume that the p -6P emission near 425 nm propagates with possible amplification only in the (widest) fibers with $b > 200\text{--}250$ nm.

The sample is photoexcited at normal incidence with the laser beam polarization set parallel to the long axis of the p -6P molecules, so that a maximum material absorption of $\approx 60\%$ is achieved. The emission is found to be rather isotropic, due to both light diffraction at the exit of the nanofibers and disorder-induced light scattering. Nevertheless, the emission features a degree of polarization (parallel to the long molecular axis) > 7 dB. Figure 2 displays a set of time-integrated emission spectra for different values of the excitation fluence. The emission is collected nearly perpendicularly to the plane of the mica substrate, but the emission collected at different angles yields similar results. When the pump fluence reaches a given threshold value, very sharp, randomly spaced lines arise at wavelengths across the 0–1 emission band of p -6P near 425 nm. Lines having a resolution-limited width (2 \AA) are observed. The line spectral distribution is strongly dependent on the excitation position on the sample surface (inset of Fig. 2). However, the spectral pattern is well reproduced in different acquisitions taken at different times, so that we exclude that the narrow lines are experimental artifacts. The threshold fluence (Φ_{th}) is as low as $0.5 \mu\text{J}/\text{cm}^2$ per pulse (incident on the sample); changes in the sample location yield variations of a factor of three in Φ_{th} . Assuming an internal conversion efficiency of 100%, for $\Phi_{\text{th}} = 0.5 \mu\text{J}/\text{cm}^2$, we estimate a threshold density (N_{th}) of $6 \times 10^{16} \text{ cm}^{-3}$. All the above-mentioned characteristics are found to be independent of temperature in the 30–300 K range; in particular, the threshold fluence remains constant within our 10% experimental accuracy.

The observed nonlinear spectra are reminiscent of “random lasing”.^{14–16} As the quantity of material deposited be-

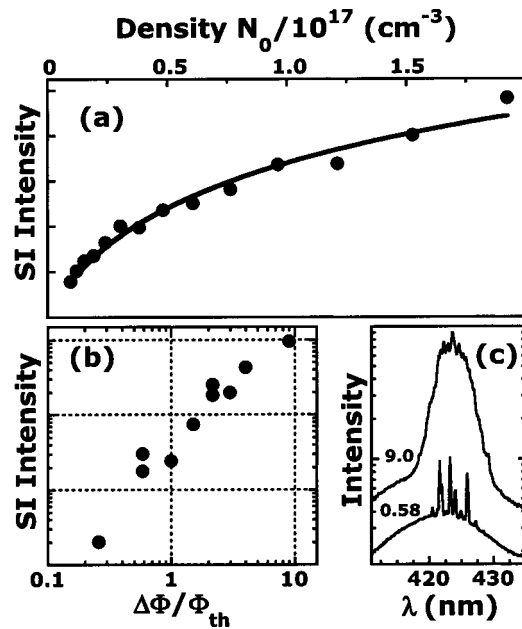


FIG. 3. Panel (a): SI emission intensity vs photoexcited density N_0 , for pump intensities below threshold ($T=30$ K). The solid dots are the experimental points and the solid line is a fit to the data using Eq. (1). Panel (b): SI random lasing plus stimulated emission intensity versus normalized pump excess fluence $\Delta\Phi/\Phi_{\text{th}}$ ($T=300$ K). Panel (c): Emission spectra recorded at $\Delta\Phi/\Phi_{\text{th}}=0.58$ and 9.0 ($T=300$ K).

tween the nanofibers is negligible, we attribute the optical feedback responsible for laser action to efficient (random) multiple scattering of light propagating along the nanofibers caused by fiber inhomogeneities. Feedback is possibly provided also by well defined end facets with good optical quality.

Figure 3(a) shows the spectrally integrated (SI) emission intensity as a function of the estimated density (N_0) excited by the ultrafast laser pulses, for densities below threshold. The data actually refer to a position on the sample with a threshold density $N_{\text{th}} = 2 \times 10^{17} \text{ cm}^{-3}$. The sublinear dependence of the signal versus N_0 indicates that threshold is achieved in the regime of (nonradiative) bimolecular recombination for the photoexcited density. An estimate of the bimolecular recombination rate can be obtained by data fitting. The time-integrated emission intensity (S_{TI}) has the form:

$$S_{\text{TI}} \propto \int N(t) dt \sim \ln \left(\frac{k_{\text{ss}} N_0}{k_0} + 1 \right), \quad (1)$$

where k_{ss} and k_0 are the bimolecular recombination rate and the (low-intensity) inverse photoluminescence lifetime, respectively. From data fitting using the expression given in Eq. (1) and $k_0 = 1.8 \times 10^9 \text{ s}^{-1}$,¹⁷ we find $k_{\text{ss}} = (0.9 \pm 0.2) \times 10^{-7} \text{ cm}^3/\text{s}$. By comparing data sets obtained in different positions on the sample, we determine that the value of k_{ss} lies in the interval $(0.3\text{--}1.1) \times 10^{-7} \text{ cm}^3/\text{s}$. The bimolecular recombination rate (and so the exciton diffusion coefficient) of crystalline p -6P are thus found to be of the same order of magnitude as that reported in literature for crystalline tetracene.¹⁸

For excitation levels just above threshold, laser action first takes place in a few nanofibers featuring efficient random feedback and long gain paths. Thanks to their narrow linewidth, random modes emerge from the intense spontane-

ous emission spectrum resulting from all the other fibers, which are characterized by higher optical losses. These latter represent the majority of the crystalline needles. The evolution of the emission spectrum as a function of the excitation power is in fact very similar to that reported in an ensemble of dye-filled microcrystals, where laser oscillation begins on a single crystal, while all the other microresonators, supporting lossier modes, contribute to the ensemble response with spontaneous emission only.¹⁹ The emission intensity for excitation levels above Φ_{th} is plotted in Fig. 3(b) as a function of the normalized pump excess fluence, defined as $\Delta\Phi/\Phi_{th} \equiv (\Phi - \Phi_{th})/\Phi_{th}$. The signal is spectrally integrated over the random lasing spectrum, after subtraction of the spontaneous emission contribution. The emission varies superlinearly with $\Delta\Phi/\Phi_{th}$. At small values of $\Delta\Phi/\Phi_{th}$, the number of oscillating modes increases with increasing pump fluence, since different random modes are characterized by different lasing thresholds,¹⁶ as a consequence, the total emission of the narrow lines increases superlinearly with increasing $\Delta\Phi/\Phi_{th}$. Eventually, ASE is achieved along nanofibers with higher optical losses and not contributing to lasing. The rise of an ASE band explains: (i) The persistence of the superlinear growth of the emission intensity¹⁵ and (ii) the progressive decrease in visibility of the random lasing modes at large values of $\Delta\Phi/\Phi_{th}$, as shown in Fig. 3(c).

In summary, we report experimental evidence of random laser action in crystalline *p*-6P consisting of self-organized nanofibers. Threshold fluences as low as $0.5 \mu\text{J}/\text{cm}^2$ ($6 \times 10^{16} \text{ cm}^{-3}$ equivalent threshold densities) are observed near 425 nm with subpicosecond pulses as the excitation source. Our studies allow for the estimate of intrinsic material parameters, such as the bimolecular recombination rate which is found to be as high as $10^{-7} \text{ cm}^3/\text{s}$.

In spite of the high *p*-6P crystalline order, the onset of density-dependent recombination processes occurs at a density which is only a factor of 2–3 lower than the lowest threshold density we observed. Moreover, a threshold density $N_{th} = 6 \times 10^{16} \text{ cm}^{-3}$ yields an equivalent threshold current density (J_{th}) of $\approx 2\text{--}3 \text{ kA}/\text{cm}^2$ in continuous-wave operation, assuming a singlet-to-triplet injection ratio of 0.3 and no additional density-dependent loss mechanisms other than bimolecular recombination. Current densities of the order of J_{th} could be sustainable in organic crystals,²⁰ suggesting that electrical pumping is potentially feasible in crystalline *p*-6P. We conclude that highly ordered oligomer crystals are very promising as gain materials for future nanoscale optoelectronic and photonic devices.

The authors acknowledge partial support from the EC RTN “Nanochannels” (Contract no. HPRN-CT-2002-00323), and the Austrian Foundation for Advancement of Scientific Research (FWF projects P-15155, P-15627, P-15629, and P-15630-N08). Part of this work was performed within the Christian Doppler Society’s dedicated laboratory on Plastic Solar Cells funded by the Austrian Ministry of Economic Affairs and Konarka Austria Ges.m.b.H. The authors would like also to thank Harald Hoppe for his help with the atomic force microscopy (AFM) measurements.

- ¹N. Tessler, G. J. Denton, and R. H. Friend, *Nature (London)* **382**, 695 (1996).
- ²M. Berggren, A. Dodabalapur, R. E. Slusher, and Z. Bao, *Nature (London)* **389**, 466 (1997).
- ³V. G. Kozlov, V. Bulović, P. E. Burrows, and S. R. Forrest, *Nature (London)* **389**, 363 (1997).
- ⁴M. D. McGehee, M. A. Díaz-García, F. Hide, R. Gupta, E. K. Miller, D. Moses, and A. J. Heeger, *Appl. Phys. Lett.* **72**, 1536 (1998).
- ⁵F. Garnier, G. Horowitz, P. Valat, F. Kouki, and V. Wintgens, *Appl. Phys. Lett.* **72**, 2087 (1998).
- ⁶H. J. Brouwer, V. V. Krasnikov, T. A. Pham, R. E. Gill, and G. Hadziioannou, *Appl. Phys. Lett.* **73**, 708 (1998).
- ⁷M. Nagawa, R. Hibino, S. Hotta, H. Yanagi, M. Ichikawa, T. Koyama, and Y. Taniguchi, *Appl. Phys. Lett.* **80**, 544 (2002).
- ⁸H. Yanagi and T. Morikawa, *Appl. Phys. Lett.* **75**, 187 (1999).
- ⁹A. Andreev, G. Matt, C. J. Brabec, H. Sitter, D. Badt, H. Seyringer, and N. S. Sariciftci, *Adv. Mater. (Weinheim, Ger.)* **12**, 629 (2000).
- ¹⁰F. Balzer and H.-G. Rubahn, *Appl. Phys. Lett.* **79**, 3860 (2001).
- ¹¹H. Yanagi, T. Ohara, and T. Morikawa, *Adv. Mater. (Weinheim, Ger.)* **13**, 1452 (2001).
- ¹²H. Plank, R. Resel, S. Purger, J. Keckes, A. Thierry, B. Lotz, A. Andreev, N. S. Sariciftci, and H. Sitter, *Phys. Rev. B* **64**, 235423 (2001); H. Plank, R. Resel, A. Andreev, N. S. Sariciftci, and H. Sitter, *J. Cryst. Growth* **237**, 2076 (2002); H. Plank, R. Resel, H. Sitter, A. Andreev, N. S. Sariciftci, G. Hlawacek, C. Teichert, A. Thierry, and B. Lotz, *Thin Solid Films* **443**, 108 (2003).
- ¹³F. Balzer, V. G. Bordo, A. C. Simonsen, and H.-G. Rubahn, *Phys. Rev. B* **67**, 115408 (2003).
- ¹⁴S. V. Frolov, Z. V. Vardeny, K. Yoshino, A. Zakhidov, and R. H. Baughman, *Phys. Rev. B* **59**, R5284 (1999).
- ¹⁵M. Anni, S. Lattante, R. Cingolani, G. Gigli, G. Barbarella, and L. Favaretto, *Appl. Phys. Lett.* **83**, 2754 (2003).
- ¹⁶H. Cao, Y. G. Zhao, S. T. Ho, E. W. Seelig, Q. H. Wang, and R. P. H. Chang, *Phys. Rev. Lett.* **82**, 2278 (1999).
- ¹⁷The value of k_0 is deduced from photoluminescence lifetime measurements made on the same nanofibers.
- ¹⁸A. J. Campillo, R. C. Hyer, S. L. Shapiro, and C. E. Swenberg, *Chem. Phys. Lett.* **48**, 495 (1977).
- ¹⁹G. Ihlein, F. Schüth, O. Krauß, U. Vietze, and F. Laeri, *Adv. Mater. (Weinheim, Ger.)* **10**, 1117 (1998).
- ²⁰M. A. Baldo, R. J. Holmes, and S. R. Forrest, *Phys. Rev. B* **66**, 035321 (2003).